ELSEVIER

Catalysis Today 74 (2002) 53–63

CATALYSIS TODAY

www.elsevier.com/locate/cattod

# Glucose hydrogenation over Ni–B/$SiO_2$ amorphous alloy catalyst and the promoting effect of metal dopants

Hui Li, Hexing Li*, Jing-Fa Deng[1]

*Department of Chemistry, Fudan University, Shanghai 200433, PR China*

**Abstract**

The Ni–B/$SiO_2$ amorphous catalyst was prepared by chemical reduction with $KBH_4$ aqueous solution. The amorphous structure was verified by XRD, EXAFS, and DSC. During the liquid phase glucose hydrogenation, the as-prepared Ni–B/$SiO_2$ amorphous catalyst exhibited much higher activity than other Ni-based catalysts, such as the corresponding crystallized Ni–B/$SiO_2$ catalyst, the Ni/$SiO_2$ catalyst obtained by $H_2$ reduction, and even the commercial Raney Ni catalyst. This was interpreted in terms of both the structural effect and the electronic effect. Effects of the preparation conditions on the activity of the Ni–B/$SiO_2$ amorphous catalyst were investigated which revealed that the maximum activity was achieved by using the 40–60 mesh $SiO_2$ support and calcining the catalyst precursor at 473 K for 2 h. Appropriate concentration of Cr-, Mo-, and W-promoters could further enhance its activity since the presence of these promoters in the low-valent state could act as Lewis adsorption sites which favored the adsorption and polarization of the carbonyl group (C=O) in the glucose molecule. However, large concentration of the promoters led to a decrease in the activity since too many Ni active sites were covered by these oxides. 

*Keywords:* Glucose; Hydrogenation; Ni–B/$SiO_2$ amorphous catalyst; Metal promoters

## 1. Introduction

The hydrogenation of glucose to sorbitol is of great industrial importance because sorbitol is a valuable polyol used as additives in foods, drugs, and cosmetics or as a synthon for the preparation of Vitamin C [1]. The most frequently used catalyst in the above hydrogenation is Raney Ni. Up to now, very few works have been reported on the liquid phase glucose hydrogenation performed over other catalysts [2]. Recently, metal-metalloid amorphous alloy catalysts caused much attention owing to their excellent activity and selectivity as well as their strong sulfur resistance in various hydrogenation reactions. Among them, the Ni–B amorphous catalysts were most thoroughly studied for the hydrogenation of the olefinic function [3–7], such as in cyclopentadiene [8–11], benzene [12–14], and acrylonitrile [15–19]. However, glucose hydrogenation over the supported Ni–B amorphous catalysts has not been reported. In this paper, a Ni–B/$SiO_2$ amorphous catalyst was prepared by chemical reduction and exhibited higher activity than other Ni-based catalysts such as the crystalline Ni–B/$SiO_2$, the Ni/$SiO_2$, and even the Raney Ni catalysts. The promoting effect of Cr-, Mo-, and W-dopants on the activity was also investigated.

## 2. Experimental

### 2.1. Catalyst preparation

The Ni–B/$SiO_2$ amorphous catalyst was prepared by regular impregnation following chemical reduction

* Corresponding author.
*E-mail address:* jfdeng@srcap.stc.sh.cn (H. Li).
[1] Author deceased.

0920-5861/02/$ – see front matter 
PII: S0920-5861(01)00530-2

with $KBH_4$ aqueous solution, as reported elsewhere [15]. A commercial silica (40–60 mesh, 185 $m^2\,g^{-1}$) was impregnated by a $NiCl_2$ aqueous solution over night. After being dried, the catalyst precursor was calcined at different temperatures from 373 to 773 K for 2 h, and then reduced by adding $KBH_4$ solution dropwise with vigorous stirring in an ice-water bath. The resulting Ni–B/$SiO_2$ sample was washed thoroughly with distilled water until free from the soluble boron species and $K^+$ or $Na^+$ ions, which may affect the activity of the catalyst [20]. It was further washed with absolute alcohol (EtOH) and finally kept in EtOH until the time of use. The crystalline Ni–B/$SiO_2$ catalyst was obtained by treating the fresh Ni–B/$SiO_2$ sample at 873 K for 2 h in $N_2$ flow. The Cr-, Mo-, and W-promoted Ni–B/$SiO_2$ catalysts were prepared using a similar method to that of the Ni–B/$SiO_2$ catalyst by adding appropriate amount of $K_2CrO_4$, or $Na_2WO_4$, or $Na_2MoO_4$ salt to the $NiCl_2$ solution. The Ni/$SiO_2$ catalyst was prepared by $H_2$ reduction at 723 K for 4 h. Raney Ni catalyst was commercially available from a sorbitol production factory in China and was used without additional activation.

### 2.2. Catalyst characterization

The content of Ni and the metal promoters (wt.%) in the unpromoted and promoted Ni–B/$SiO_2$ catalysts and the bulk composition of these catalysts (at.%) were analyzed by inductively coupled plasma (ICP, Jarrell-As Scan 2000). The active surface area ($S_{act}$) was determined by hydrogen chemisorption using a dynamic pulse method. The catalyst surface was purged in a helium stream (purity of 99.997%, treated with a Chrompack clean-oxygen filter) at 573 K for 2 h. Crystallization of the catalyst should be carefully avoided during the pretreatment. After the catalyst was cooled down to room temperature in a helium stream, hydrogen pulses were injected continuously until the calculated area of the consecutive pulses was constant. According to hydrogen chemisorption, the $S_{act}$ of the catalysts was calculated assuming H/Ni(s) = 1 and a surface area of $6.5 \times 10^{-20}$ $m^2$ per Ni atom [21]. Experimental error was determined as less than 10%. The amorphous structure of Ni–B/$SiO_2$ catalysts was determined by both the X-ray powder diffraction (XRD, Bruker AXS D8-Advance with Cu Kα radiation) and the extended X-ray absorption fine structure (EXAFS, 4W1B in Beijing Synchrotron Radiation Facility, China). The crystallization process was followed by differential scanning calorimetry (DSC, Perkin–Elmer) under $N_2$ atmosphere at a heating rate of 10 K $min^1$. The surface morphology was observed by a scanning electron micrograph (SEM, XL 30 Philips). X-ray photoelectron spectroscopy (XPS) was performed on a Perkin–Elmer PHI 5000C ESCA system to determine the surface electronic states of the catalysts. All the binding energy values were calibrated using C 1s = 284.6 eV as a reference.

### 2.3. Activity test

Liquid phase hydrogenation of glucose was performed at 373 K and 4.0 MPa in a stainless steel autoclave, which contained 3.0 g of catalyst and 50 ml 50% (w/w) of glucose aqueous solution. During the hydrogenation, the reaction mixture was stirred vigorously to eliminate the diffusion effects [1]. The time of hydrogenation over each of the catalysts was 6 h in order to compare the glucose conversion. The reaction products were analyzed by a gas chromatograph equipped with a 25 m OV 101 capillary column and a FID, in which the oven temperature was programmed at a ramping rate of 4 K $min^{-1}$ from 353 to 533 K. The catalysts were found to be highly selective in the hydrogenation of glucose with almost no by-prouducts. After reaction for 6 h the reaction conversion was obtained by determining the remained glucose in the mixture with Fehlings agent, as described elsewhere [7].

## 3. Results and discussion

### 3.1. Preliminary study of reaction kinetics

Preliminary rate measurements were performed on the fresh Ni–B/$SiO_2$ catalyst. First, the dependence of the rate upon the stirring speed was studied, which revealed that there was a plateau above 1000 rpm, where the rate did not depend on the stirring speed. Therefore, a standard stirring speed of 1200 rpm was used subsequently. At such a stirring speed, the dependence of glucose conversion (after reaction for 6 h) on the amount of the Ni–B/$SiO_2$ amorphous catalyst

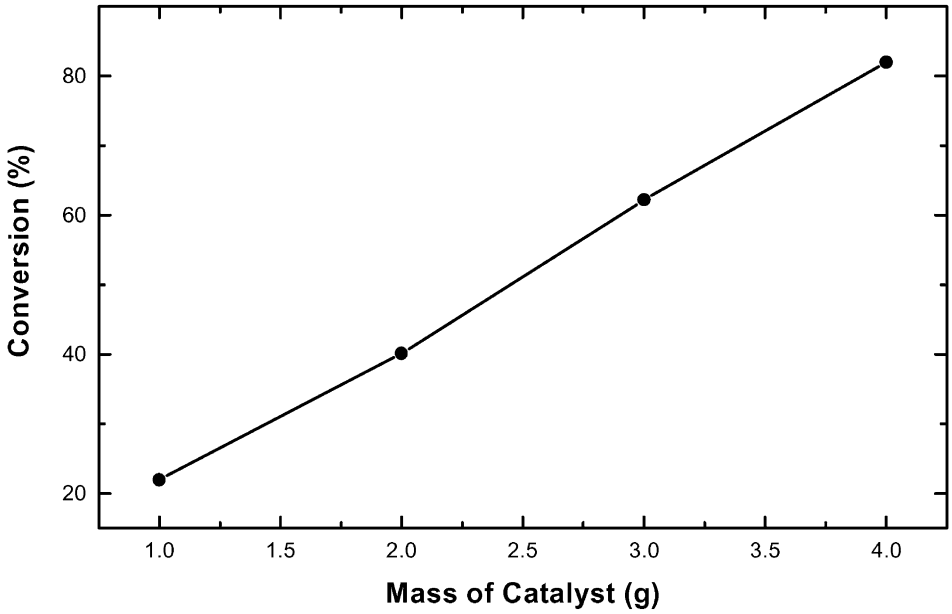


Fig. 1. Dependence of the reaction conversion on the mass of Ni–B/$SiO_2$(6.4 wt.% Ni) during the glucose hydrogenation. The reaction conditions: 50 ml 50%(w/w) glucose aqueous solution, $T = 373$ K, $P_{H_2} = 40$ MPa, stirring speed = 1200 rpm.

(6.4 wt.% Ni) is shown in Fig. 1. The proportional relationship clearly demonstrated the absence of external mass transfer limitation. However, the above results could not rule out the possible internal diffusion limitation. Therefore, the size of the $SiO_2$ support should be carefully selected. As shown in Table 1, the Ni–B/$SiO_2$ catalyst exhibited the highest activity by using $SiO_2$ support with the size of 40–60 mesh and remained nearly constant when the size of the support was further decreased, indicating that the internal diffusion limitation was essentially eliminated.

Table 1
Effect of the $SiO_2$ size on the activity of Ni–B/$SiO_2$ catalyst with Ni loading of 10.1 wt.% Ni[a]

| Size (mesh) | Conversion (%) |
|---|---|
| 20–40 | 62.63 |
| 40–60 | 82.47 |
| 60–80 | 79.51 |
| 80–100 | 80.24 |

[a] Reaction conditions: 3.0 g catalyst, 50 ml 50% (w/w) glucose aqueous solution, $T = 373$ K, $P_{H_2} = 40$ MPa, stirring speed = 1200 rpm.

To obtain the maximum activity of the as-prepared Ni–B/$SiO_2$ catalyst, the effect of the pretreatment of the catalyst precursor was also investigated. As shown in Fig. 2, the activity first increased and then decreased with the increase of the calcination temperature. The lower activity of the catalyst obtained at low calcination temperature was mainly attributed to the poor interaction between the Ni active sites and the support, resulting in the low content of Ni active sites, since a part of them were leached away during the $BH_4^-$ reduction in aqueous solution. At high calcination temperatures, the activity of Ni–B/$SiO_2$ catalyst also decreased since the interaction between $Ni^{2+}$ ions and the support was too strong which resulted in a low reduction degree of the catalyst. As reported previously [15], the reduction degree of the Ni–B/$SiO_2$ catalyst played a key role for its activity. Therefore, 473 K was chosen as an optimum calcination temperature.

Since the glucose hydrogenation rate changed linearly with the $P_{H_2}$ from 1.0 to 5.0 MPa and remained almost unchanged with the glucose concentration, it could be concluded that, the reaction was first order with respect to hydrogen and zero

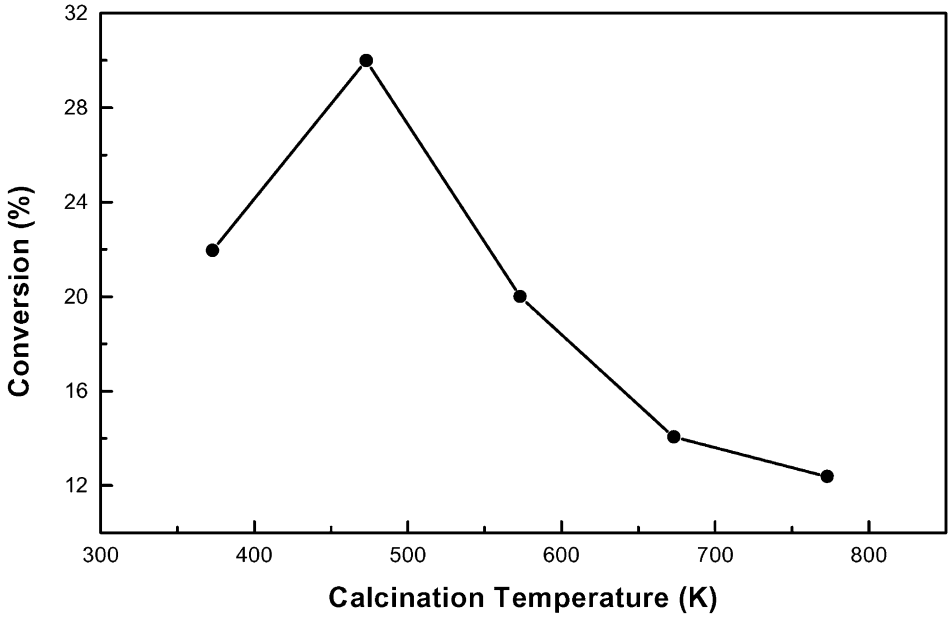


Fig. 2. Effect of the calcination temperature of the catalyst precursor on the activity of Ni–B/$SiO_2$(6.4 wt.% Ni) amorphous catalyst in glucose hydrogenation. Reaction conditions: 1.0 g catalyst was employed and other conditions are given in Fig. 1.

order with respect to glucose concentration. This could be understood by considering the saturated adsorption of glucose molecules and the unsaturated adsorption of hydrogen on the catalyst surface [1].

### 3.2. Unpromoted Ni–B/$SiO_2$ amorphous catalyst

The amorphous structure of the as-prepared Ni–B/$SiO_2$ sample was determined by XRD patterns, as shown in Fig. 3. For the fresh Ni–B/$SiO_2$ sample,

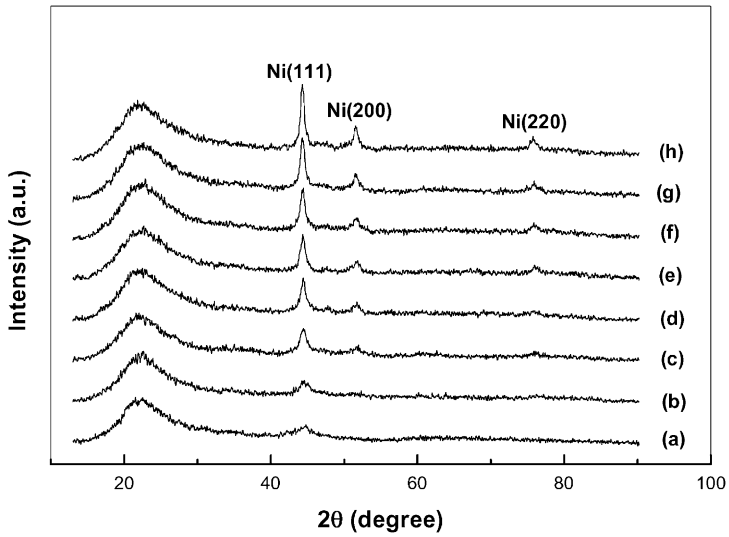


Fig. 3. In situ XRD patterns of Ni–B/$SiO_2$ (a) 523 K; (b) 573 K; (c) 623 K; (d) 673 K; (e) 723 K; (f) 773 K; (g) 823 K; (h) 873 K.

besides a small peak around $2\theta = 22^\circ$ corresponding to the amorphous $SiO_2$, only one broad peak around $2\theta = 45^\circ$ was observed, indicating a typical amorphous structure [22,23]. When the Ni–B/$SiO_2$ sample was treated at an elevated temperature, the in situ XRD patterns revealed that the crystallization of the sample occurred at a temperature around 623 K. Both the number and the intensity of the diffraction peaks increased with the increase of the treating temperature, showing the occurrence of the crystallization process. However, no significant peaks corresponding to the crystalline Ni–B alloy were observed. This was partly due to the decomposition of Ni–B alloy at high temperature and also to the spillover of the residual Ni–B alloy on the support. The unsupported Ni–B amorphous alloy demonstrated the presence of the crystalline Ni–B alloy phase when it was treated at high temperatures, as shown in Fig. 4. The amorphous structure was further confirmed by EXAFS on $\chi(k)k^3$ Ni edge, from which the RDF curves could be obtained by the fast Fourier transformation. As shown in Fig. 5, only one FT peak around $R = 2.0$ Å was observed for the fresh Ni–B/$SiO_2$ sample, indicating that it had no long-range but only short-range ordered structure [24]. The shoulder peak was indicative of the alloying B. When it was treated at elevated temperatures, the intensity of the original peak gradually increased and finally, two small additional peaks appeared at longer distance, showing the transformation of the Ni–B alloy from the amorphous structure to ordered crystalline structure. In addition, as shown in Fig. 6, the DSC analysis demonstrated that the Ni–B/$SiO_2$ amorphous catalyst crystallized via two steps corresponding to temperatures of 694 and 782 K, respectively.

Fig. 7 shows the XPS spectra of the fresh Ni–B/$SiO_2$ and the corresponding crystallized samples. In comparison with the spectra of standard substances shown in Fig. 7, one can conclude that the peaks at 188.2 and 192.7 eV in B 1s level of the fresh sample are ascribed to the elemental boron and oxidized boron, which was similar to that found in unsupported Ni–B amorphous alloy. In Ni $2p_{3/2}$ level, both the metallic Ni at BE of 852.6 eV and the oxidized Ni at BE of 855.8 eV were also observed. Since no oxidized Ni species were observed in the unsupported Ni–B sample, it could be concluded that some Ni species can not be reduced by $BH_4^-$ in the presence of silica support due to the interaction between the $Ni^{2+}$ ions and the support. In comparison with the standard BE values of pure metallic Ni and amorphous boron powder [16], it was found that the BE of the alloying B shifted positively about 1.1 eV. This implied that partial electron transfer from alloying B to metallic Ni,

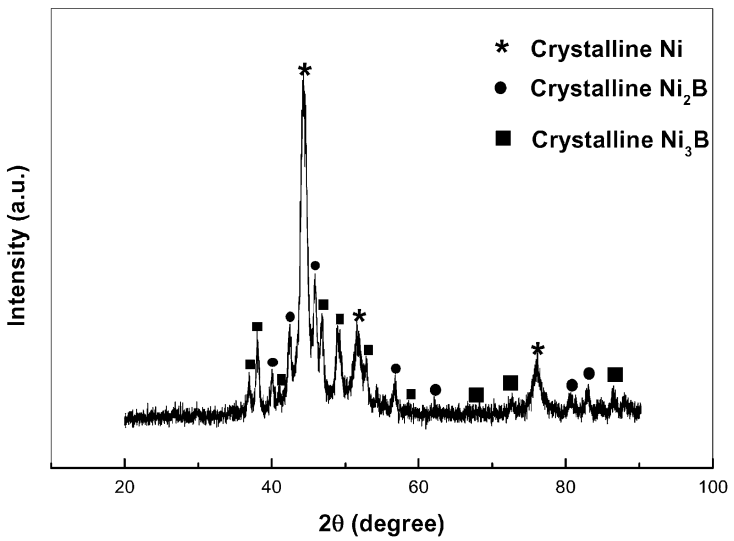


Fig. 4. XRD pattern of the crystallized Ni–B sample obtained by in situ heating treatment of the ultrafine Ni–B amorphous alloy sample.

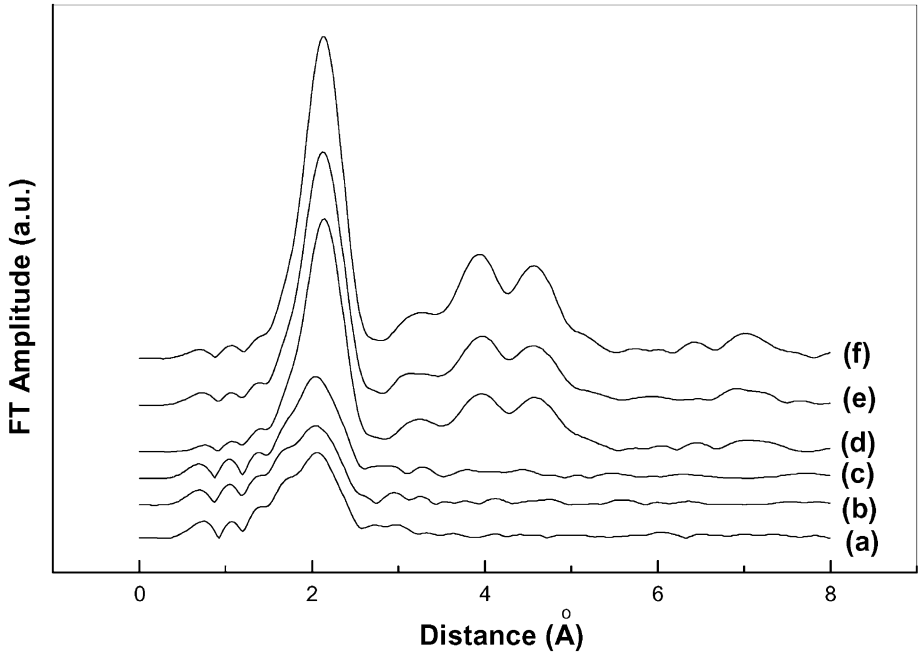


Fig. 5. RDF curves of the Ni–B/$SiO_2$ catalyst treated in situ at elevated temperatures. (a) 373 K; (b) 473 K; (c) 573 K; (d) 673 K; (e) 773 K; (f) 873 K.

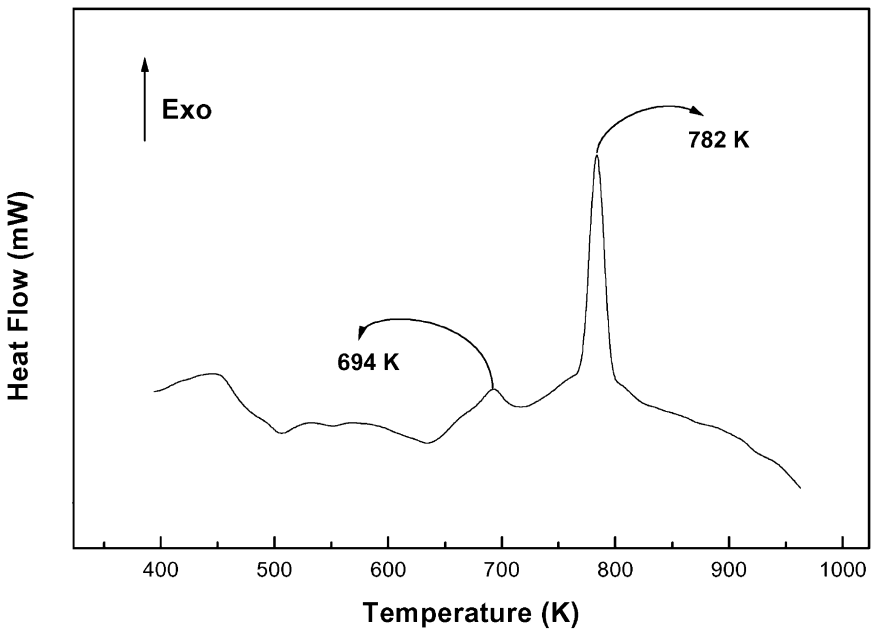


Fig. 6. DSC curve of the Ni–B/$SiO_2$ amorphous catalyst.

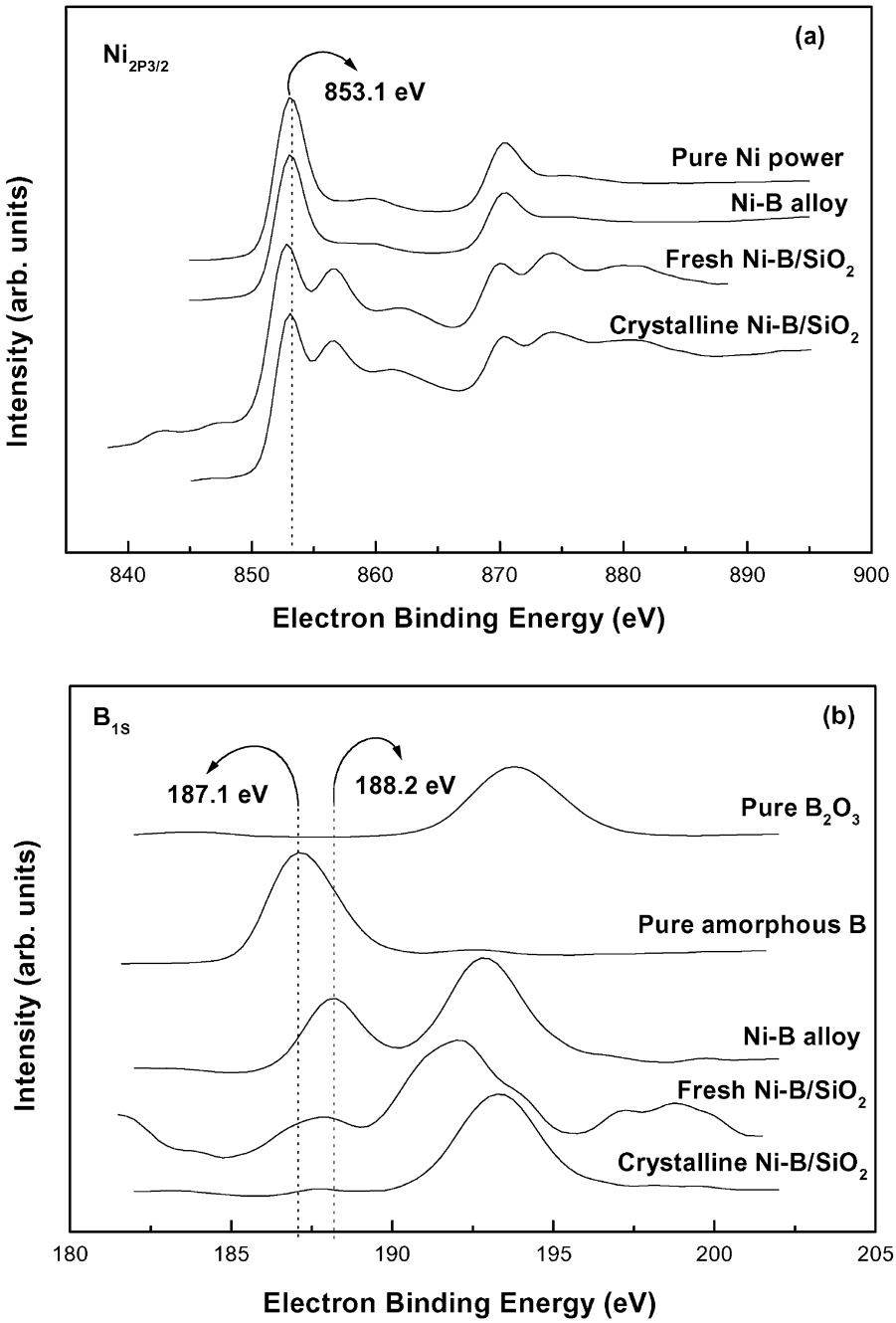


Fig. 7. XPS spectra of Ni–B sample and its relative substances. (a) Ni $2p_{3/2}$; (b) B 1s.

making Ni electron-rich. The failure to observe the BE shift of metallic Ni in Ni–B alloy was possibly due to the big size of Ni atom in comparison with that of B [16]. After being treated at high temperature, the BE of the metallic Ni was almost the same as that of pure Ni. It was also found that most of the B species in the crystallized Ni–B/$SiO_2$ sample were present in the oxidized state, possibly due to the deep oxidation of these alloying boron species by trace oxygen in the $N_2$ flow.

The SEM micrographs of the Ni–B/$SiO_2$ sample during in situ heat treatment is shown in Fig. 8. It can be seen that the fresh sample exhibited a cotton-like surface morphology composed of small particles with an average size around 80–100 nm. These particles gradually gathered when the sample was treated at elevated temperatures, resulting in big lumps in the SEM micrographs.

Table 2 gives the glucose conversions over various catalysts. The glucose reaction over Ni–B/$SiO_2$ amorphous catalyst could repeat for more than 5 cycles without considerable decrease in its activity and only less than 1.0 ppm Ni in the product mixture was detected by ICP, showing the excellent durability of the Ni–B/$SiO_2$ amorphous catalyst. The most representative value of catalyst activity is turnover frequency (TOF), which is expressed as the number of glucose molecules converted per second on per surface Ni site.

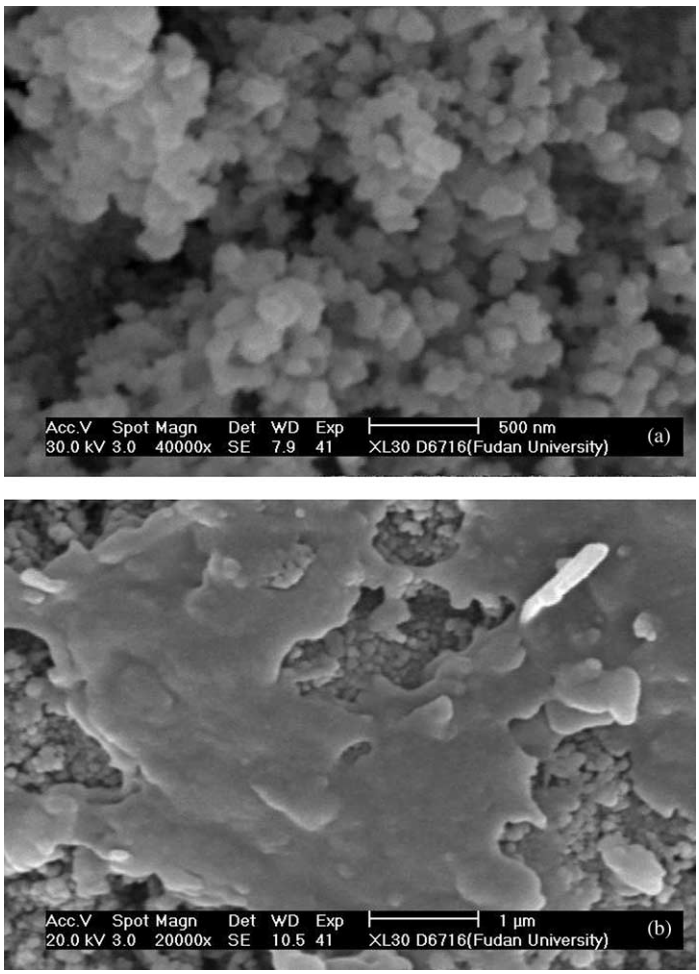


Fig. 8. SEM morphologies of (a) the fresh Ni–B/$SiO_2$ sample and (b) the Ni–B/$SiO_2$ sample after being treated at 873 K in $N_2$ flow for 2 h.

Table 2
Hydrogenation activities of different catalysts[a]

| Catalyst | Mass (g) | Ni loading (wt.%) | $S_{act}$ ($m^2$/g·Ni) | Reaction time (h) | Conversion (%) | TOF ($s^{-1}$) |
|---|---|---|---|---|---|---|
| Ni–B/$SiO_2$(fresh) | 1.0 | 6.4 | 32.6 | 6.0 | 30.00 | 0.0240 |
| Ni–B/$SiO_2$(873 K)[b] | 1.0 | 6.4 | 20.4 | 6.0 | 14.20 | 0.0181 |
| Ni/$SiO_2$ | 1.0 | 10 | 24.0 | 6.0 | 7.76 | 0.0084 |
| Raney Ni | 1.0 | – | 43.0 | 6.0 | 22.30 | 0.0135 |

[a] Reaction conditions are the same as given in Table 1.
[b] After being treated at 873 K for 2 h in $N_2$ flow.

As shown in Table 2, the Ni–B/$SiO_2$ amorphous alloy catalyst exhibited higher activity than other Ni-based catalysts, such as the Ni/$SiO_2$ catalyst obtained by $H_2$ reduction at high temperature, the corresponding Ni–B/$SiO_2$ crystalline catalyst obtained by treating the fresh Ni–B/$SiO_2$ sample at 873 K for 2 h in $N_2$ flow, and the Raney Ni catalyst commercially available from a sorbitol production factory in China.

Several factors could account for the higher activity of the Ni–B/$SiO_2$ amorphous catalyst. First, as can be seen from Table 2, it had a larger active area ($S_{act}$) in comparison with the crystalline Ni–B/$SiO_2$ and Ni/$SiO_2$ catalysts. However, the $S_{act}$ is only 37 and 26% larger respectively in Ni–B/$SiO_2$ amorphous catalyst than in the crystallized Ni–B/$SiO_2$ and Ni/$SiO_2$ catalysts, which can not account for the 53 and 74% activity enhancement. Furthermore, it also can not account for the higher glucose conversion over the Ni–B/$SiO_2$ amorphous catalyst than that over Raney Ni which had higher $S_{act}$ and more Ni (noting that the Ni loading in Ni–B/$SiO_2$ amorphous catalyst was only 6.4 wt.%). Therefore, the promoting of both the structural characteristics and surface electronic state of the Ni–B/$SiO_2$ amorphous catalyst should be considered to explain its excellent activity. The structural effect could be attributed to its unique amorphous characteristics, such as the high concentration of coordinately unsaturated sites and the strong corporation between Ni active sites. According to the calculation of the EXAFS data [25], the Ni atoms in Ni–B/$SiO_2$ amorphous catalyst had a lower coordination number ($N_{Ni–Ni} = 9.8$) and shorter Ni–Ni bonding length ($R_{Ni–Ni} = 0.217$ nm) in comparison with the crystalline samples ($N_{Ni–Ni} = 11.0$, $N_{Ni–Ni} = 0.250$ nm). Those factors have been claimed to be favorable for most of the hydrogenation reaction [3]. The electronic effect was mainly attributed to the electron donation of alloying B to metallic Ni in the Ni–B amorphous alloy, making Ni electron-rich. This may weaken the adsorption for glucose molecule via the donation of a lone electron pair from the oxygen of the carbonyl group and thus favor the competitive adsorption of hydrogen against the C=O group. Therefore, more hydrogen could be adsorbed on the Ni–B/$SiO_2$ amorphous catalyst which in turn enhanced its hydrogenation activity. As mentioned above, the glucose hydrogenation was first order with respect to hydrogen and zero order with respect to glucose, showing that the adsorption of glucose was excess while the adsorption of hydrogen was limited. The above assumption was supported by the fact that the crystalline Ni–B/$SiO_2$ catalyst exhibited higher activity than that of Ni/$SiO_2$ owing to the electronic interaction between metallic Ni and alloying B which was present in the crystalline form.

### 3.3. Promoted Ni–B/$SiO_2$ amorphous catalysts

The XRD patterns revealed that the addition of Cr-, Mo-, and W-promoters did not cause significant change in the amorphous structure of the Ni–B/$SiO_2$ samples. XPS spectra demonstrated the similar surface electronic states of metallic Ni and alloying B to those of the unpromoted Ni–B/$SiO_2$ amorphous catalyst. XPS spectra also revealed that all the Cr species were present in $Cr^{3+}$ oxide ($Cr_2O_3$) and most of W or Mo species were present in $W^{4+}$ or $Mo^{3+}$ oxides ($WO_2$ and $Mo_2O_3$).

Fig. 9 shows the dependence of glucose conversion on the content of Cr-, Mo-, and W-promoters (wt.%). It can be seen that the activity of all of these promoted Ni–B/$SiO_2$ amorphous catalysts have maximum

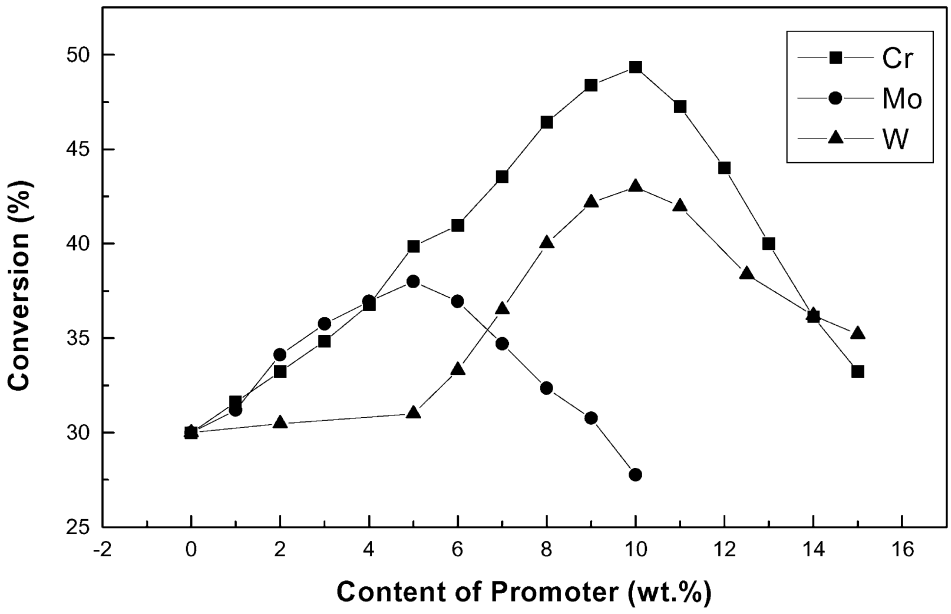


Fig. 9. Dependence of reaction conversion on the content of (a) Cr-, (b) Mo-, and (c) W-promoters during the glucose hydrogenation over the metal-doped Ni–B/$SiO_2$ amorphous catalysts with Ni loading of 6.4 wt.%. The reaction conditions are given in Fig. 2.

values with the increase of the promoter content. The optimum contents of Cr-, Mo-, and W-promoters were 10, 5, and 10 wt.%, respectively. At their individual optimum content, the promoting effect followed the order as Cr > W > Mo.

To interpret the effects of Cr-, Mo-, and W-promoters, a concerted mechanism of activation and hydrogenation of the carbonyl function similar to that proposed earlier for aldehyde hydrogenation [1,26,27] was employed which involved the association on the catalyst surface of Ni active sites and low-valent Cr, Mo, and W ions. The glucose was assumed to be adsorbed by catalyst in the equilibrium between the pyranic form and the linear form. The $Cr^{3+}$, $Mo^{3+}$, or $W^{4+}$ species could act as Lewis adsorption sites, the glucose molecule being adsorbed via the donation of lone electron pair from the oxygen of carbonyl group. This bonding polarized the C=O bond which was favorable for a nucleophilic attack on the carbon atom by hydrogen dissociatively adsorbed on neighboring Ni active sites. It was reasonable that the presence of both the Ni active sites for hydrogen adsorption (Ni-H) and the surface $Cr^{3+}$, $Mo^{3+}$, and $W^{4+}$ species for C=O adsorption was in favor of high activity in glucose hydrogenation and the maximum activity should correspond to an optimum surface concentration of these promoters. However, a large concentration of the promoters was harmful to the activity because too many surface Ni active sites would be covered by $Cr^{3+}$, $Mo^{3+}$, or $W^{4+}$ species.

## 4. Conclusion

The present work supplied a novel and powerful Ni–B/$SiO_2$ amorphous catalyst prepared by chemical reduction, which showed the potential in the industrial sorbitol production via glucose hydrogenation. Besides the high dispersion of the as-prepared Ni–B/$SiO_2$ amorphous catalyst, its high activity was mainly attributed to its favorable structural characteristics and the electronic interaction between metallic Ni and the alloying B in the Ni–B alloy which made Ni electron-rich. Addition of the Cr-, Mo-, and W-promoters could further enhance the activity of Ni–B/$SiO_2$ amorphous catalyst due to the adsorption and polarization of the carbonyl group by these promoters present in their low-valent states.

## Acknowledgements

This work is supported by the Major State Basic Research Development Program (G2000048009) and the National Natural Science Foundation of China (20073008).

## References

[1] P. Gallezot, P.J. Cerino, B. Blanc, G. Fleche, P. Fuertes, J. Catal. 146 (1994) 93.
[2] J. Volf, J. Pasek, Stud. Surf. Sci. Catal. 27 (1986) 105.
[3] A. Baiker, Faraday Discuss. Chem. Soc. 87 (1989) 239.
[4] A. Molnar, G.V. Smith, M. Bartok, Adv. Catal. 36 (1989) 329.
[5] J.F. Deng, H. Li, W.J. Wang, Catal. Today 51 (1999) 113.
[6] Y. Chen, Catal. Today 44 (1998) 3.
[7] H. Li, H.X. Li, W. Wang, J.F. Deng, Chem. Lett. (1999) 629.
[8] W.J. Wang, M.H. Qiao, H.X. Li, J.F. Deng, Appl. Catal. A 166 (1998) 243.
[9] W.J. Wang, M.H. Qiao, J. Yang, S.H. Xie, J.F. Deng, Appl. Catal. A 63 (1997) 101.
[10] W.J. Wang, M.H. Qiao, H.X. Li, J.F. Deng, J. Chem. Technol. Biotechnol. 72 (1998) 280.
[11] W.J. Wang, H.X. Li, S.H. Xie, Y.J. Li, J.F. Deng, Appl. Catal. A 184 (1998) 33.
[12] H.X. Li, H.Y. Chen, S.Z. Dong, J.F. Deng, Appl. Surf. Sci. 125 (1998) 115.
[13] H.M. Wang, Z.B. Yu, H.Y. Chen, J. Yang, J.F. Deng, Appl. Catal. A 129 (1995) 143.
[14] S.H. Xie, M.H. Qiao, H.X. Li, W.J. Wang, J.F. Deng, Appl. Catal. A 176 (1999) 129.
[15] H. Li, H.X. Li, J.F. Deng, Appl. Catal. A 193 (2000) 9.
[16] H. Li, H.X. Li, J.F. Deng, Appl. Surf. Sci. 152 (1999) 25.
[17] H. Li, H.X. Li, J.F. Deng, Appl. Catal. A 207 (2001) 151.
[18] S.H. Xie, H.X. Li, H. Li, J.F. Deng, Appl. Catal. A 189 (1999) 45.
[19] Z.B. Yu, M.H. Qiao, H.X. Li, J.F. Deng, Appl. Catal. A 163 (1997) 1.
[20] P. Marginean, A Olariu, Appl. Catal. A 140 (1996) 59.
[21] J.J.F. Scholten, A.P. Pijers, A.M.L. Hustings, Catal. Rev.-Sci. Eng. 27 (1985) 151.
[22] H. Yamashita, M. Yonezawa, T. Funabiki, S. Yoshida, J. Chem. Soc., Faraday Trans. I 82 (1986) 1771.
[23] H. Yamashita, M. Yonezawa, T. Funabiki, S. Yoshida, J. Chem. Soc., Faraday Trans. I 81 (1985) 2485.
[24] J.A. Schwarz, C. Contescu, A. Contescu, Chem. Rev. 95 (1995) 477.
[25] B.R. Shen, S.Q. Wei, K.N. Fan, J.F. Deng, Appl. Phys. A 65 (1997) 295.
[26] P. Gallezot, A. Giroir-Fendler, D. Richard, in: W.E. Pascoe (Ed.), Catalysis of Organic Reactions, Marcel Dekker, New York, 1992.
[27] C.D. Bellefon, P. Fouilloux, Catal. Rev.-Sci. Eng. 36 (1994) 459.